Cold-inducible RNA-binding protein (Cirp) interacts with Dyrk1b/Mirk and promotes proliferation of immature male germ cells in mice

Tomoko Masuda[a], Katsuhiko Itoh[a,1], Hiroaki Higashitsuji[a], Hisako Higashitsuji[a], Noa Nakazawa[a], Toshiharu Sakurai[a], Yu Liu[a], Hiromu Tokuchi[a], Takanori Fujita[a], Yan Zhao[a], Hiroyuki Nishiyama[b], Takashi Tanaka[c], Manabu Fukumoto[d], Masahito Ikawa[e], Masaru Okabe[e], and Jun Fujita[a,1]

[a]Department of Clinical Molecular Biology, Graduate School of Medicine, Kyoto University, Kyoto 606-8507, Japan; [b]Department of Urology, Graduate School of Comprehensive Human Sciences, University of Tsukuba, Tsukuba 3058575, Japan; [c]Department of Molecular Genetics, Graduate School of Medicine, Kyoto University, Kyoto 606-8507, Japan; [d]Department of Pathology, Institute of Development, Aging, and Cancer, Tohoku University, Sendai 980-8575, Japan; and [e]Department of Experimental Genome Research, Genome Information Research Center, Osaka University, Osaka 565-0871, Japan

Edited by Ralph L. Brinster, University of Pennsylvania, Philadelphia, PA, and approved May 24, 2012 (received for review December 30, 2011)

Cold-inducible RNA-binding protein (Cirp) was the first cold-shock protein identified in mammals. It is structurally quite different from bacterial cold-shock proteins and is induced in response to mild, but not severe, hypothermia. To clarify the physiological function of Cirp in vivo, we produced *cirp*-knockout mice. They showed neither gross abnormality nor defect in fertility, but the number of undifferentiated spermatogonia was significantly reduced and the recovery of spermatogenesis was delayed after treatment with a cytotoxic agent, busulfan. Cirp accelerated cell-cycle progression from G0 to G1 as well as from G1 to S phase in cultured mouse embryonic fibroblasts. Cirp directly bound to dual-specificity tyrosine-phosphorylation–regulated kinase 1B (Dyrk1b, also called Mirk) and inhibited its binding to p27, resulting in decreased phosphorylation and destabilization of p27. Cirp did not affect binding of Dyrk1b to cyclin D1 but inhibited phosphorylation of cyclin D1 by Dyrk1b, resulting in cyclin D1 stabilization. In the spermatogonial cell line GC-1spg, suppression of Cirp expression increased the protein level of p27, decreased that of cyclin D1, and decreased the growth rate, which depended on Dyrk1b. Consistent changes in the protein levels of p27 and cyclin D1 as well as the percentage of cells in G0 phase were observed in undifferentiated spermatogonia of *cirp*-knockout mice. In undifferentiated spermatogonia of wild-type mice, Cirp and Dyrk1b colocalized in the nucleus. Thus, our study demonstrates that Cirp functions to fine-tune the proliferation of undifferentiated spermatogonia by interacting with Dyrk1b.

In most mammals, the testes are located in the scrotum, wherein the temperature is below that of the body cavity by 2 °C to 7 °C (1). Scrotal testes become aspermatogenic if their temperature is raised to body temperature or above, either by artificial heat or by retaining them in the abdomen (2, 3). We previously identified the first mammalian cold-shock protein in the testis and named it cold-inducible RNA-binding protein (Cirp, also called Cirbp or hnRNP A18) (4). It is constitutively expressed in the male germ cells and inducibly expressed in almost all cell types by lowering the culture temperature to 32 °C but not below 20 °C. Expression of Cirp is also induced by cellular stresses such as UV irradiation and hypoxia (5–7). In response to the stress, Cirp migrates from the nucleus to cytoplasm and affects expression of its target mRNAs (8, 9). Cirp affects cell growth and protects cells from damages induced by tumor necrosis factor α, genotoxic stress, or cryptorchidism (4, 10–13).

In an adult mouse testis, spermatogenesis is sustained by germ-line stem cells (A_{single}) that undergo mitosis and self-renew or differentiate into committed A_{paired} and $A_{aligned}$ spermatogonia, which are collectively called undifferentiated spermatogonia (14). Undifferentiated spermatogonia constitute the smallest population, less than 1%, of total testicular cells, include cells with stem-cell function, and differentiate into differentiating spermatogonia (A_{1-4}, intermediate, and B), which will undergo meiosis after the final mitosis (15, 16). Recently, methods to enrich undifferentiated spermatogonia by flow cytometry using combinations of markers such as c-Kit and α6-integrin and the side population phenotype have been developed (17, 18).

Dual-specificity tyrosine-phosphorylation–regulated kinase 1B (Dyrk1b, also called Mirk) is a member of the conserved Dyrk/minibrain family of tyrosine-regulated, arginine-directed serine/threonine protein kinases (19). The highest level of Dyrk1b mRNA is observed in the testis and skeletal muscle, and Dyrk1b protein mediates muscle differentiation, cell survival, and cell migration (19). Biochemical analysis has revealed that Dyrk1b phosphorylates and blocks degradation of the cyclin-dependent kinase (CDK) inhibitor p27 in nontransformed cells that helps to maintain a quiescent state (20). Dyrk1b blocks quiescent cells from traversing G1 phase of the cell cycle by phosphorylating and destabilizing cyclin D1 and cyclin D3 (21).

In the present study, we have generated Cirp-deficient mice to clarify the biological function of mammalian cold-shock protein in vivo. We found that Cirp interacts with Dyrk1b and that it is required to fully maintain the undifferentiated spermatogonia.

Results

Number of Undifferentiated Spermatogonia Is Decreased in Cirp-Deficient Mice. We generated Cirp-deficient mice by homologous recombination in ES cells (Fig. 1*A*). Intercrossing of heterozygous mutant mice generated progeny at nearly Mendelian ratios ($cirp^{+/+}$:$cirp^{+/-}$:$cirp^{-/-}$ = 58:110:47, n = 215), and $cirp^{-/-}$ mice were indistinguishable from wild-type littermates in appearance. When we examined fertility of $cirp^{-/-}$ male mice by mating them with wild-type females, the litter size (average = 5.1 mice, n = 18) was not different from that of wild-type mating (average = 4.9 mice, n = 15). We observed no reproductive defect in $cirp^{-/-}$ females, either. Although the testis of $cirp^{-/-}$ mice looked histologically normal and the numbers of total testicular cells and differentiating spermatogonia as well as the size and weight of the testis were comparable to wild type, the percentage and number of c-Kit$^-$ and highly α6-integrin$^+$ undifferentiated spermatogonia in the

Author contributions: K.I. and J.F. designed research; T.M., K.I., Hiroaki Higashitsuji, Hisako Higashitsuji, N.N., T.S., Y.L., H.T., T.F., Y.Z., T.T., M.F., M.I., and M.O. performed research; T.M., K.I., H.N., and J.F. analyzed data; and T.M., K.I., M.O., and J.F. wrote the paper.

The authors declare no conflict of interest.

This article is a PNAS Direct Submission.

[1]To whom correspondence may be addressed. E-mail: jfujita@virus.kyoto-u.ac.jp or katsu@virus.kyoto-u.ac.jp.

This article contains supporting information online at www.pnas.org/lookup/suppl/doi:10.1073/pnas.1121524109/-/DCSupplemental.

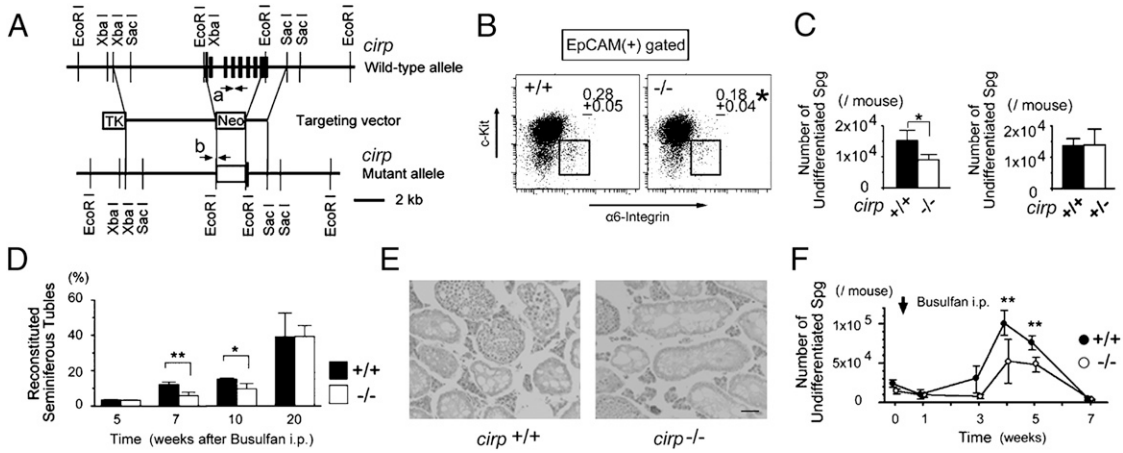

Fig. 1. Reduced number of undifferentiated spermatogonia in *cirp*-knockout mice. (*A*) Targeted disruption of the *cirp* gene. Structures of the wild-type allele, targeting vector, and mutant allele are shown together with the relevant restriction sites. The filled rectangles indicate the exons of the *cirp* gene. Neo, TK, and arrows (a and b) indicate a pgk-neo selection cassette, a thymidine kinase cassette, and the locations of primers for genomic PCR, respectively. (*B*) Flow cytometric analysis of undifferentiated spermatogonia. The fractions of undifferentiated spermatogonia (boxed) were compared between wild-type (+/+) and *cirp*-knockout (–/–) mice. *Significantly different from +/+ mice ($P < 0.05$). Data are from four +/+ and three –/– 12-wk-old mice. (*C*) Numbers of undifferentiated spermatogonia in +/+, –/–, and heterozygous knockout (+/–) mice. Significant decrease (*$P < 0.05$) was seen in –/– mice but not in +/– mice ($P = 0.93$). Values represent mean ± SD. Data are from eight +/+, three –/–, and four +/– mice. (*D*) Percentage of reconstituted seminiferous tubules after busulfan treatment. *Significantly different ($P < 0.05$). **Significantly different ($P < 0.01$). Values are mean ± SD ($n = 3$ each). (*E*) Histological sections of the testes at 7 wk after busulfan treatment. Sections are stained with hematoxylin and eosin. (Scale bar: 50 μm.) (*F*) Numbers of undifferentiated spermatogonia after busulfan treatment. ● and ○ indicate the numbers in +/+ and –/– mice, respectively. Values represent mean ± SD ($n = 3$–7). **Significantly different between +/+ and –/– mice ($P < 0.01$).

testicular epithelial cell adhesion molecule $(EpCAM)^+$ cells (18, 22) were decreased in $cirp^{-/-}$ mice compared with those in wild-type mice ($P < 0.05$) (Fig. 1 *B* and *C*). The number of undifferentiated spermatogonia in $cirp^{+/-}$ mice, however, was not different from that in wild-type mice ($P = 0.925$).

To determine whether the observed decrease in the number of undifferentiated spermatogonia has biological meaning, we analyzed the recovery process of spermatogenesis after i.p. injection of the alkylating agent busulfan (30 mg/kg body weight). The percentage of seminiferous tubules showing spermatogenesis was less than 3% and not different between wild-type and $cirp^{-/-}$ mice at 5 wk after the injection (Fig. 1*D*). At 7 and 10 wk, however, significantly fewer tubules were reconstituted in $cirp^{-/-}$ mice compared with wild-type mice (Fig. 1*E*). Consistently, the number of undifferentiated spermatogonia was significantly less in $cirp^{-/-}$ mice at 4 and 5 wk after the busulfan treatment (Fig. 1*F*).

To assess whether stem cells of other cell lineages are affected by deficiency of Cirp, we analyzed purified bone marrow cells enriched with hematopoietic stem cells (23, 24). Their numbers were comparable between $cirp^{-/-}$ and wild-type mice (Fig. S1 *A* and *B*). The competitive reconstitution assay did not reveal any significant difference between them even with an additional irradiation of recipient mice (Fig. S1 *C* and *D*). In contrast to spermatogonia, *cirp* mRNA expression was barely detectable in the analyzed hematopoietic cells (Fig. S1*E*).

Cirp Accelerates Cell-Cycle Progression in Cultured Mouse Embryonic Fibroblasts (MEFs). To analyze the effect of Cirp in vitro, we made several MEF cell lines that inducibly change the protein level of Cirp (Fig. S2 *A* and *B*). As shown in Fig. 2*A*, $cirp^{-/-}$ MEFs proliferated faster when Cirp was expressed both at 32 °C and 37 °C. When expression of Cirp was suppressed by shRNAs at 32 °C, proliferation of $cirp^{+/+}$ MEFs was suppressed (Fig. 2*B*). The suppressive effect was reversed by expression of shRNA-insensitive Cirp construct (Fig. S2 *C* and *D*), suggesting that the observed effect was not attributable to off-target effects of shRNAs.

We next analyzed the effect of Cirp on the cell cycle by BrdU incorporation and propidium iodide staining. When exogenous Cirp was expressed in $cirp^{-/-}$ MEFs at 32 °C, the percentage of cells in G0/G1 phase was reduced and that in S phase increased significantly (Fig. 2*C*). Conversely, when expression of Cirp was suppressed in $cirp^{+/+}$ MEFs at 32 °C, the percentage of cells in G0/G1 phase was increased and that in S phase reduced significantly (Fig. 2*C*). The changes in the Cirp protein levels did not affect the percentage of the sub-G1 population (Fig. S3*A*). These results indicate that expression of Cirp accelerates the G0/G1-to-S phase transition without affecting apoptosis.

The cells with 2N DNA content and that are not positively stained with anti-Ki67 antibody are considered to be in the G0 phase of the cell cycle (25). The G0 state is characterized by significantly decreased ribosomal RNA synthesis and lowered total cellular protein content. When Cirp was expressed in $cirp^{-/-}$ MEFs, the percentage of cells in the fraction of $Ki67^{low}$ or $Ki67^-$ was significantly decreased, and the percentage of cells highly positive for pyronin Y staining, which stains polysomal RNA, was increased (Fig. 2*D*). Conversely, the percentage of G0 cells was significantly increased when Cirp expression was suppressed in $cirp^{+/+}$ MEFs at 32 °C (Fig. 2*E*). These results demonstrate that Cirp accelerates cell-cycle progression from G0 to G1 as well as from G1 to S phase in cultured MEFs.

Cirp Binds to Dyrk1b and Inhibits Its Kinase Activity. Yeast two-hybrid screening of a mouse testis cDNA library using Cirp as bait suggested that the C-terminal glycine-rich domain of Cirp binds to Dyrk1b (Fig. S4*A*).

When exogenously expressed as GFP-fusion proteins in HEK293T cells, full-length Cirp and its glycine-rich domain, but not its N-terminal RNA-binding domain, were coimmunoprecipitated with Dyrk1b as expected (Fig. S4 *B* and *C*). The region of Dyrk1b that interacted with Cirp was the kinase domain (Fig. S4*D*). Binding of endogenous Cirp and Dyrk1b was detected in MEFs of the $cirp^{+/+}$ genotype cultured at 32 °C (Fig. S4*E*). The recombinant Cirp protein bound to recombinant Dyrk1b protein in vitro, indicating a direct interaction

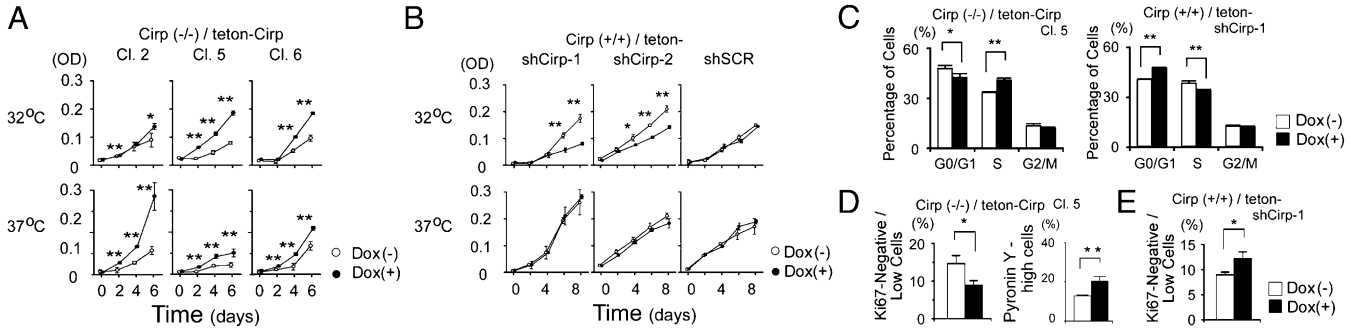

Fig. 2. Accelerated proliferation of MEFs expressing Cirp. (*A* and *B*) Effects of Cirp on cell growth. Cells from Cirp(−/−)/teton-Cirp clones 2, 5, and 6 (Cl. 2, Cl. 5, and Cl. 6, respectively) were derived from *cirp*$^{-/-}$ MEFs that express Cirp in the presence of Dox. Cirp(+/+)/teton-shCirp cells were derived from *cirp*$^{+/+}$ MEFs that Dox-inducibly express shRNAs that knockdown Cirp expression (shCirp-1 and shCirp-2) or scrambled RNAs (shSCR). Cells were cultured in the presence (+) or absence (−) of Dox at the indicated temperatures. Cell numbers were assessed by 3-(4,5-dimethylthiazol-2-yl)-2,5-diphenyltetrazolium bromide (MTT) assays. Values are mean ± SD (n = 3 or 4). *P < 0.05. **P < 0.01. (*C*) Analysis of the cell cycle by flow cytometry. BrdU incorporation and DNA content were analyzed in indicated cells cultured at 32 °C in the presence (+) or absence (−) of Dox. Percentages of cells in indicated phases of cell cycle are shown. Values are mean ± SD (n = 3). *P < 0.05. **P < 0.01. (*D* and *E*) Percentages of cells in G0 phase in the presence (+) or absence (−) of Dox. Ki67 expression, stainability with pyronin Y, and DNA content were analyzed in indicated cells by flow cytometry. Values are mean ± SD (n = 3). *P < 0.05.

(Fig. S4*F*). Immunocytochemistry demonstrated that Cirp was induced and colocalized with Dyrk1b in the nucleus at 32 °C in *cirp*$^{+/+}$ MEFs (Fig. S4*G*). In undifferentiated and differentiating spermatogonia, Cirp and Dyrk1b mRNAs were expressed, and their proteins were colocalized in the nucleus (Fig. S4 *H* and *I*).

Dyrk1b phosphorylates p27 and cyclin D1 to affect cell-cycle progression (19). When increasing amounts of Cirp were expressed in HEK293T cells, decreasing amounts of p27 were coimmunoprecipitated with Dyrk1b (Fig. 3*A*). In contrast, the amount of cyclin D1 coimmunoprecipitated with Dyrk1b was not decreased in the presence of Cirp and its binding to Dyrk1b (Fig. S5*A*). The presence of cyclin D1 did not affect the binding of Cirp to Dyrk1b either, and Cirp was coimmunoprecipitated with cyclin D1 as well (Fig. S5 *B* and *C*). These results indicate that Cirp forms a complex together with Dyrk1b and cyclin D1.

Dyrk1b immunoprecipitated from HEK293T cells could phosphorylate recombinant p27 in vitro (Fig. 3*B*). The amount of phosphorylated p27 was dose-dependently decreased in the presence of Cirp. When we incubated recombinant cyclin D1 with recombinant Dyrk1b, phosphorylation of cyclin D1 was observed (Fig. 3*C*). The phosphorylation was dose-dependently suppressed by Cirp. Interestingly, Cirp was also phosphorylated by Dyrk1b.

These data demonstrate that Cirp binds to and inhibits the kinase activity of Dyrk1b toward both p27 and cyclin D1, although Cirp competitively blocks the binding of Dyrk1b to p27 but not to cyclin D1.

Effects of Cirp on Cell-Cycle Progression Are Mediated by p27 and Cyclin D1 via Dyrk1b. Rapid removal of p27 at the G0/G1 transition and expression of cyclin D1 at the G1/S transition are required for effective progression of the cell cycle to S phase (26, 27). When Cirp was inducibly expressed with doxycycline (Dox) in *cirp*$^{-/-}$ MEFs, expression of p27 was decreased and that of cyclin D1 was increased (Fig. 4*A*) because of the increased and decreased degradation rates of p27 and cyclin D1, respectively (Fig. S4 *J* and *K*). Conversely, when expression of Cirp was suppressed in *cirp*$^{+/+}$ MEFs, expression of p27 was increased and that of cyclin D1 was decreased (Fig. 4*A*).

Because p27 and cyclin D1 are known to be phosphorylated by kinases besides Dyrk1b (26, 27), we examined whether the effects of Cirp on p27 and cyclin D1 depended on Dyrk1b. We stably expressed shRNAs targeted to Dyrk1b mRNAs or scrambled shRNAs in *cirp*$^{-/-}$ MEFs that inducibly express Cirp (Fig. S5*D*). Induction of Cirp decreased the protein level of p27

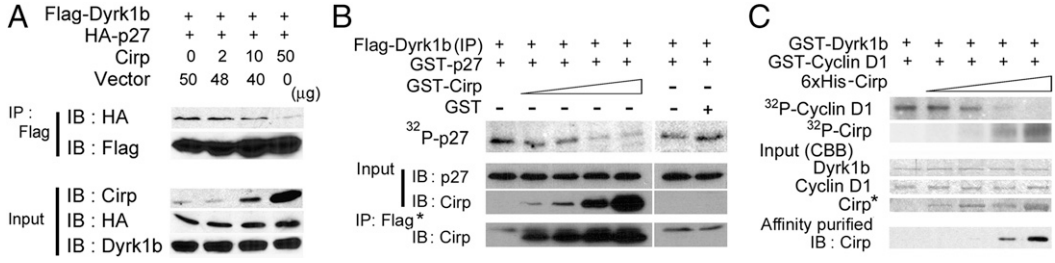

Fig. 3. Inhibition of Dyrk1b kinase activity by Cirp. (*A*) Effects of Cirp on binding of p27 to Dyrk1b. Plasmids were cotransfected into HEK293T cells as indicated. Proteins immunoprecipitated (IP) with anti-FLAG antibody and inputs were analyzed by Western blotting (IB) using the indicated antibodies. +, Present; −, absent. (*B*) Effects of Cirp on in vitro kinase activity of Dyrk1b toward p27. Immunoprecipitants (IP) were prepared from HEK293T cells expressing FLAG-Dyrk1b by using anti-FLAG antibody. Their kinase activity was assayed in the presence of [γ-^{32}P]ATP, GST-p27, and increasing amounts of GST-Cirp or GST. Reaction mixtures were separated by SDS/PAGE and analyzed by autoradiography. Proteins coprecipitated with protein G Sepharose beads (*) from the reaction mixtures without ^{32}P and inputs (2%) were analyzed by IB using the indicated antibodies. (*C*) Effects of Cirp on in vitro kinase activity of Dyrk1b toward cyclin D1. Recombinant GST-Dyrk1b was incubated with [γ-^{32}P]ATP, GST-cyclin D1, and increasing amounts of His-tagged Cirp and analyzed as in *B*. The lower images show Coomassie blue staining (CBB) of the indicated proteins used in the assay and IB of proteins coprecipitated with glutathione Sepharose beads from the reaction mixtures without ^{32}P (affinity-purified). *1/4 of input. Experiments were repeated three (*A*) and four (*B* and *C*) times, with similar results.

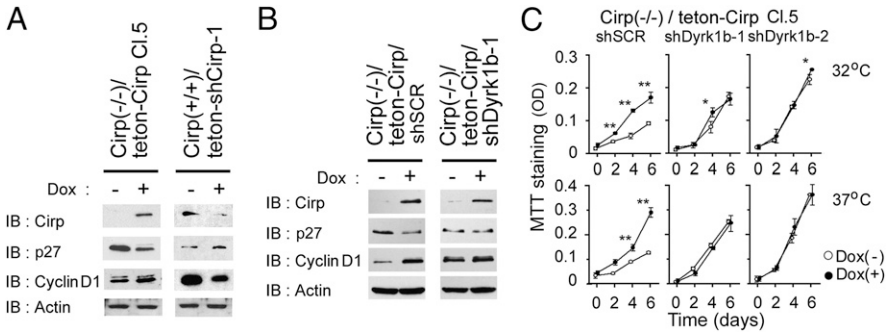

Fig. 4. Effects of Cirp on p27 and cyclin D1 via Dyrk1b in cultured MEFs. (*A*) Effects of Cirp on p27 and cyclin D1 protein levels. Cirp(–/–)/teton-Cirp Cl. 5 and Cirp(+/+)/teton-shCirp-1 cells were cultured at 32 °C in the presence (+) or absence (–) of Dox. Cell lysates were analyzed by IB using the indicated antibodies. (*B*) Dyrk1b dependency of protein levels. Indicated cells, both derived from Cirp(–/–)/teton-Cirp Cl. 5 cells, were cultured at 37 °C and analyzed as in *A*. (*C*) Dyrk1b and cell growth. Indicated cells were cultured at 32 °C and 37 °C in the presence (+) or absence (–) of Dox. Cell numbers were assessed by MTT assays. Values are mean ± SD (n = 3). *$P < 0.05$. **$P < 0.01$. Experiments were repeated four (*B*) and three (*C*) times, with similar results.

and increased that of cyclin D1 in *cirp*$^{-/-}$ MEFs expressing scrambled shRNAs (Fig. 4*B* and Fig. S5*E*). When expression of Dyrk1b was suppressed, however, Cirp did not show these effects in *cirp*$^{-/-}$ MEFs. The growth rate of these cells was not affected by Cirp either (Fig. 4*C*). These data demonstrate that expression of Cirp accelerates cell-cycle progression by inhibiting the kinase activity of Dyrk1b toward p27 and cyclin D1 in MEFs.

Down-Regulation of Cirp Suppresses Cell-Cycle Progression in a Spermatogonial Cell Line in Vitro and Undifferentiated Spermatogonia in Vivo. To analyze the effect of Cirp on male germ cells, we first used the mouse spermatogonial cell line GC-1spg (28). When GC-1spg cells were transduced with control retrovirus expressing scrambled shRNAs, expression of Cirp was induced at 32 °C like parental cells (Fig. S6*A*). In GC-1spg cells transduced with retrovirus expressing shRNAs to *cirp* mRNAs, the induction of Cirp was partly suppressed, the level of p27 protein was increased, and the level of cyclin D1 protein was decreased (Fig. S6*B*). These cells proliferated more slowly than the control cells (Fig. 5*A*). To confirm that growth-suppressive effect of Cirp down-regulation depends on Dyrk1b, we further down-regulated Dyrk1b expression (Fig. S6*C*). As shown in Fig. 5*B*, the impaired growth was rescued by suppressing the expression of Dyrk1b.

Next, we examined the effects of Cirp deficiency on the cell cycle in undifferentiated spermatogonia in vivo. At 4 wk after injection of busulfan, the percentage of Ki67^{+} cells was significantly smaller and the percentage of pyronin Y^{low} cells was significantly larger in undifferentiated spermatogonia isolated from *cirp*$^{-/-}$ mice than those from *cirp*$^{+/+}$ wild-type mice (Fig. 5*C*). RT-PCR analysis demonstrated that undifferentiated spermatogonia expressed mRNAs for p27 and cyclin D1 (Fig. 5*D*) as well as for Cirp and Dyrk1b. Furthermore, the protein level of p27 was higher and that of cyclin D1 was lower in undifferentiated spermatogonia of *cirp*$^{-/-}$ mice compared with those of wild-type mice, although the mRNA level for p27 was not different and that for cyclin D1 was higher in *cirp*$^{-/-}$ mice (Fig. 5*E* and Fig. S7 *A* and *B*). Altogether, these data indicate that Cirp destabilizes p27 and stabilizes cyclin D1 at the protein level in undifferentiated spermatogonia, resulting in an accelerated cell-cycle progression in wild-type mice and decreased proliferation in Cirp-deficient mice.

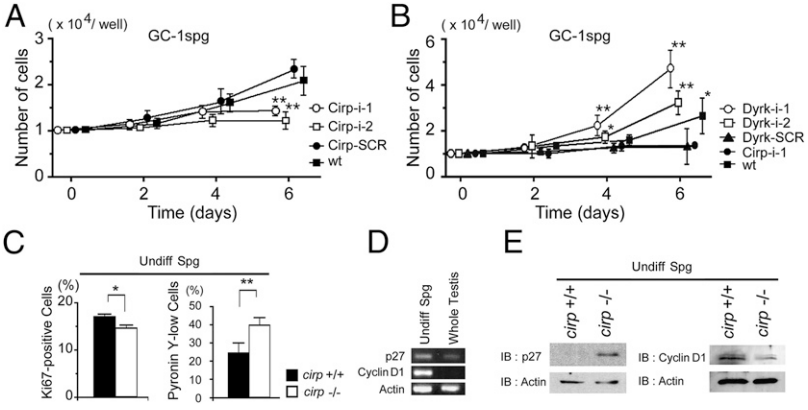

Fig. 5. Impaired cell-cycle progression in Cirp-deficient spermatogonia. (*A*) Effects of Cirp on growth of cultured GC-1spg cells. Cells were transduced with retrovirus [murine stem cell virus-LTRmiR30-PIG (MSCV-LMP)] expressing RNAi sequences targeted to Cirp (Cirp-i-1 and Cirp-i-2) or scrambled sequence (Cirp-SCR). Cells were cultured at 32 °C, and cell numbers were assessed by MTT assays. wt, untransduced cells. Values are mean ± SD (n = 3). **$P < 0.01$. (*B*) Dyrk1b-dependent effects of Cirp on growth of GC-1spg cells. Cirp-i-1 cells were further transduced with retrovirus [Friend spleen focus-forming virus-based hybrid vector 2 (SF2)] expressing RNAi sequences targeted to Dyrk1b (Dyrk-i-1 and Dyrk-i-2) or scrambled sequence (Dyrk-SCR) and analyzed as in *A*. (*C*–*E*) Undifferentiated spermatogonia of *cirp*$^{-/-}$ and *cirp*$^{+/+}$ genotypes were sorted and analyzed at 4 wk after busulfan treatment. (*C*) The percentages of Ki67^{+} (*Left*) and pyronin Y^{-} or pyronin Y^{low} (*Right*) cells were assessed by flow cytometry. Values are mean ± SD [n = 3 (*Left*) or 4 (*Right*)]. *$P < 0.05$ and **$P < 0.01$, respectively, different between wild-type (+/+) and *cirp*-knockout (–/–) mice. (*D*) Detection of p27 and cyclin D1 transcripts in spermatogonia isolated from *cirp*$^{-/-}$ mice. cDNAs were analyzed by RT-PCR. (*E*) Protein levels of p27 and cyclin D1. Cell lysates were analyzed by IB using the indicated antibodies. Experiments were repeated three times (*D* and *E*), with similar results.

Discussion

Numbers and Proliferative Activity of Undifferentiated Spermatogonia Are Decreased in *cirp*-Knockout Mice. In mammals, there have been only two established cold-shock proteins reported to date, Cirp and RNA-binding motif protein 3 (Rbm3), which are structurally quite similar (5). In the mouse testis, Cirp is constitutively expressed in the germ cells and the level varies depending on the stage of differentiation, whereas Rbm3 is suggested to be expressed mainly in the Sertoli cells (3, 29). When mouse testis is exposed to heat stress, expression of Cirp and Rbm3 is decreased, suggesting that the decreased expression might be related to the heat-induced testicular damage. Indeed, overexpression of Cirp has recently been reported to reduce the damage by cryptorchidism (13). In the present study, we found that the Cirp-deficient mice have reduced numbers of undifferentiated spermatogonia, although the total numbers of testicular germ cells and fertility were not significantly decreased. When they were exposed to the cytotoxic agent busulfan, the recovery of spermatogenesis was affected slightly but significantly. In addition to Cirp, Rbm3 was expressed in spermatogonia (Fig. S7 *C* and *D*). Because its expression level was not increased in spermatogonia of the *cirp*$^{-/-}$ genotype compared with those of wild type, it seems unlikely that the relatively mild defects observed in the knockout mice are a consequence of redundancy/compensation by Rbm3. Analysis of the *cirp* and *rbm3* double-knockout mice would clarify this possibility.

A vast majority of stem cell functions reside in the undifferentiated spermatogonia population (30). The findings that the undifferentiated spermatogonia expressed Cirp and that proliferation of the spermatogonial cell line was suppressed when Cirp expression was decreased suggest that the observed defect in *cirp*$^{-/-}$ mouse testis is mainly intrinsic to the spermatogonia rather than their environment. Consistent with this notion, no effect of Cirp deficiency was observed in hematopoietic stem cell populations that normally do not express Cirp.

Cells overexpressing Cirp are more resistant to various stresses, and down-regulation of Cirp inhibits cell growth in some cancer cells (31). We found that cell-cycle progression is inhibited at both G1-to-S and G0-to-G1 phase transitions with no change in the sub-G1 population in Cirp-deficient MEFs. Consistently, the proportion of undifferentiated spermatogonia in G0 phase was increased in *cirp*$^{-/-}$ mice compared with wild-type mice after treatment with busulfan. The numbers of apoptotic testicular cells were not apparently different between *cirp*$^{-/-}$ and wild-type mice after busulfan treatment, and the sensitivity of cultured MEFs of the *cirp*$^{-/-}$ genotype to busulfan was not affected by expression of Cirp (Fig. S3 *B* and *C*). In addition, expression of Cirp stimulated proliferation of the spermatogonial cell line. Thus, the decrease in the number of undifferentiated spermatogonia in *cirp*$^{-/-}$ mice could be considered mainly attributable to decreased cell proliferation rather than increased cell death.

The growth-stimulatory effects of Cirp on spermatogonia and MEFs seem contradictory to our original finding in BALB/3T3 cells (4) and consistent with the finding in CHO cells (32). We have also observed growth-suppressive effects of Cirp in NIH/3T3 and U-2 OS cells (Fig. S8*A*). Growth-stimulatory effects have been observed by others in PC3 and LNCaP human prostate cancer cells and MEFs, but not in NIH/3T3, HeLa, IMR90, or human mammary epithelial cells (10, 12). These two classes of cell lines that differently respond to Cirp expression were not distinguished by the protein levels of cyclin D1, CDK inhibitors such as p16 and p27, Dyrk1b, or Cirp (Fig. S8 *B* and *C*). Further studies are thus necessary to clarify this issue. Cirp probably fine-tunes the proliferation of cells by promoting and suppressing growth signals through distinct protein–protein and protein–RNA interactions, which depend on multiple factors, including the cell types, stresses, and conditions of cells.

Cirp Binds to and Inhibits the Kinase Activity of Dyrk1b Toward p27 and Cyclin D1. Dyrk1b autophosphorylates the second tyrosine in the Tyr-X-Tyr motif, an event that is essential for full kinase activity (33). Once phosphorylated, Dyrk1b functions as a serine/threonine kinase. Ran-binding protein M (RanBPM) directly binds to Dyrk1b and inhibits its kinase activity toward hepatocyte nuclear factor 1α (HNF1α) (34). In contrast, direct binding to dimerization cofactor of HNF1 from muscle (DCoHm) potentiates Dyrk1b's activity as an activator of HNF1α (35). Although phosphorylation of RanBPM or DCoHm by Dyrk1b has not been detected (34), we found that Cirp directly binds to and is phosphorylated by Dyrk1b, resulting in inhibition of its kinase activity toward p27 and cyclin D1.

p27 opposes cell-cycle progression by inhibiting cyclin E/Cdk2 (27). The expression level of p27 is high during G0 phase but decreases rapidly on reentry of the cells into G1 phase. Ser^{10} is the major site of p27 phosphorylation by Dyrk1b in resting cells that leads to protein stability (20). Previous studies have suggested a role of p27 in male germ-cell development. Mice deficient in S-phase kinase-associated protein 2 (Skp2), which mediates ubiquitin-dependent degradation of p27, exhibit a progressive loss in spermatogenic cells (36). Conversely, testes from p27-knockout mice are significantly larger (37) and contain increased numbers of type A spermatogonia (38), and EpCAM^{+} spermatogonia from the knockout mice proliferate more actively than those from wild-type mice do (39). We found that Cirp decreases the protein level of p27 and increases cell proliferation via Dyrk1b in MEFs and the spermatogonial cell line and that the p27 protein level and cells in G0 phase were increased in Cirp-deficient undifferentiated spermatogonia. These results strongly suggest that the absence of Cirp increases phosphorylation of p27 by Dyrk1b, resulting in its stabilization and reduced cell-cycle progression in undifferentiated spermatogonia of the *cirp*$^{-/-}$ genotype.

D-type cyclins are G1-specific cyclins that associate with Cdk4 or Cdk6 and promote restriction point progression during G1 phase (40). In accordance with the immunohistochemical study by Beumer et al. (41), we detected expression of cyclin D1 in undifferentiated spermatogonia. The protein level of cyclin D1 was decreased in undifferentiated spermatogonia of *cirp*$^{-/-}$ mice compared with wild-type mice. Although binding to Cirp decreases the activity of Dyrk1b to phosphorylate cyclin D1 as well as to p27, the binding inhibits the binding of Dyrk1b to p27 but not to cyclin D1. After phosphorylation by Dyrk1b, p27 remains a functional CDK inhibitor, does not translocate from the nucleus, and colocalizes with Dyrk1b in G0 (20). Mitogen stimulation then causes cells to enter G1, reduces Dyrk1b levels (42), and initiates the translocation of p27 to the cytoplasm to be degraded. Thus, induction at moderately low temperatures, colocalization in the nucleus with Dyrk1b, and inhibition of Dyrk1b's binding to p27 would contribute to the ability of Cirp to enhance degradation of p27. Cyclin D1 is translocated into the cytoplasm during S phase, where it is destroyed by the proteasome after phosphorylation at Thr^{286} by glycogen synthase kinase 3. Dyrk1b phosphorylates cyclin D1 at Thr^{288}, which also enhances its rapid turnover (26). The nuclear complex formation of Dyrk1b, Cirp, and cyclin D1 would thus inhibit the nuclear export and degradation of cyclin D1. Although Cirp itself is a substrate and seems to compete with cyclin D1 for phosphorylation (Fig. 3*C*), it is also possible that Cirp has an independent mechanism for inhibiting Dyrk1b activity. The precise molecular mechanism by which Cirp inhibits the kinase activity of Dyrk1b remains to be elucidated.

In summary, we have demonstrated unique physiological function of the mammalian cold-shock protein Cirp that might

partly explain why testis should be kept cool. Cirp fine-tunes the cell-cycle progression of undifferentiated spermatogonia as well as fibroblasts and cancer cells by interacting with and suppressing kinase activity of Dyrk1b to modulate the protein levels of p27 and cyclin D1 (Fig. S9). Because Cirp affects proliferation of immature male germ cells and could act as an oncoprotein in some tumors, these findings may pave the way for development of new diagnoses and treatments for male infertility and cancers.

Materials and Methods

Generation of the Targeting Vector. The 6.4-kb XbaI/EcoRI fragment of the genomic DNA clones of the *cirp* locus (Fig. 1*A*) was inserted between the neomycin-resistance cassette and the HSV thymidine kinase gene, both of which are driven by the phosphoglycerate kinase 1 (PGK1) promoter, in the pPNT vector. The 1.4-kb EcoRI/SacI fragment was inserted upstream of the neomycin-resistance gene (Fig. 1*A*).

Isolation of Undifferentiated Spermatogonia. Isolation of undifferentiated spermatogonia was performed as described by Takubo et al. (18) with minor modifications.

Additional materials and experimental procedures are provided in *SI Materials and Methods*.

ACKNOWLEDGMENTS. We thank Dr. C. Toniatti and Dr. H. Bujard for the Bs/IRES-M2 plasmid; Dr. T. Shinohara, Dr. M. Sugai, and Dr. R. J. Mayer for helpful comments; and Dr. K. Nonoguchi for technical assistance. This work was supported in part by the Smoking Research Foundation of Japan, the Cooperative Research Project Program at the Institute of Development, Aging, and Cancer at Tohoku University; and Grants-in-Aid for Scientific Research (KAKENHI) from the Japan Society for the Promotion of Science.

1. Harrison RG, Weiner JS (1948) Abdomino-testicular temperature gradients. *J Physiol* 107:48–49.
2. Carrick F, Setchell B (1977) The evolution of the scrotum. *Reproduction and Evolution*, eds Calaby J, Tyndale-Biscoe T (Australian Academy of Science, Canberra), pp 165–170.
3. Nishiyama H, et al. (1998) Decreased expression of cold-inducible RNA-binding protein (CIRP) in male germ cells at elevated temperature. *Am J Pathol* 152:289–296.
4. Nishiyama H, et al. (1997) A glycine-rich RNA-binding protein mediating cold-inducible suppression of mammalian cell growth. *J Cell Biol* 137:899–908.
5. Fujita J (1999) Cold shock response in mammalian cells. *J Mol Microbiol Biotechnol* 1:243–255.
6. Wellmann S, et al. (2004) Oxygen-regulated expression of the RNA-binding proteins RBM3 and CIRP by a HIF-1-independent mechanism. *J Cell Sci* 117:1785–1794.
7. Yang C, Carrier F (2001) The UV-inducible RNA-binding protein A18 (A18 hnRNP) plays a protective role in the genotoxic stress response. *J Biol Chem* 276:47277–47284.
8. De Leeuw F, et al. (2007) The cold-inducible RNA-binding protein migrates from the nucleus to cytoplasmic stress granules by a methylation-dependent mechanism and acts as a translational repressor. *Exp Cell Res* 313:4130–4144.
9. Yang R, Weber DJ, Carrier F (2006) Post-transcriptional regulation of thioredoxin by the stress inducible heterogenous ribonucleoprotein A18. *Nucleic Acids Res* 34: 1224–1236.
10. Sakurai T, et al. (2006) Cirp protects against tumor necrosis factor-alpha-induced apoptosis via activation of extracellular signal-regulated kinase. *Biochim Biophys Acta* 1763:290–295.
11. Artero-Castro A, et al. (2009) Cold-inducible RNA-binding protein bypasses replicative senescence in primary cells through extracellular signal-regulated kinase 1 and 2 activation. *Mol Cell Biol* 29:1855–1868.
12. Zeng Y, Kulkarni P, Inoue T, Getzenberg RH (2009) Down-regulating cold shock protein genes impairs cancer cell survival and enhances chemosensitivity. *J Cell Biochem* 107:179–188.
13. Zhou KW, Zheng XM, Yang ZW, Zhang L, Chen HD (2009) Overexpression of CIRP may reduce testicular damage induced by cryptorchidism. *Clin Invest Med* 32:E103–E111.
14. Meistrich ML, van Beek MEAB (1993) Spermatogonial stem cells. *Cell and Molecular Biology of the Testis*, eds Desjardins C, Ewing LL (Oxford Univ Press, Oxford, UK), pp 266–294.
15. Nakagawa T, Nabeshima Y, Yoshida S (2007) Functional identification of the actual and potential stem cell compartments in mouse spermatogenesis. *Dev Cell* 12:195–206.
16. Oatley JM, Brinster RL (2006) Spermatogonial stem cells. *Methods Enzymol* 419:259–282.
17. Barroca V, et al. (2009) Mouse differentiating spermatogonia can generate germinal stem cells in vivo. *Nat Cell Biol* 11:190–196.
18. Takubo K, et al. (2008) Stem cell defects in ATM-deficient undifferentiated spermatogonia through DNA damage-induced cell-cycle arrest. *Cell Stem Cell* 2:170–182.
19. Friedman E (2007) Mirk/Dyrk1B in cancer. *J Cell Biochem* 102:274–279.
20. Deng X, Mercer SE, Shah S, Ewton DZ, Friedman E (2004) The cyclin-dependent kinase inhibitor p27(Kip1) is stabilized in G(0) by Mirk/dyrk1B kinase. *J Biol Chem* 279: 22498–22504.
21. Deng X, Ewton DZ, Friedman E (2009) Mirk/Dyrk1B maintains the viability of quiescent pancreatic cancer cells by reducing levels of reactive oxygen species. *Cancer Res* 69:3317–3324.
22. Anderson R, Schaible K, Heasman J, Wylie C (1999) Expression of the homophilic adhesion molecule, Ep-CAM, in the mammalian germ line. *J Reprod Fertil* 116: 379–384.
23. Osawa M, Hanada K, Hamada H, Nakauchi H (1996) Long-term lymphohematopoietic reconstitution by a single CD34-low/negative hematopoietic stem cell. *Science* 273:242–245.
24. Harrison DE (1980) Competitive repopulation: A new assay for long-term stem cell functional capacity. *Blood* 55:77–81.
25. Kubbutat MH, et al. (1994) Epitope analysis of antibodies recognising the cell proliferation associated nuclear antigen previously defined by the antibody Ki-67 (Ki-67 protein). *J Clin Pathol* 47:524–528.
26. Alao JP (2007) The regulation of cyclin D1 degradation: Roles in cancer development and the potential for therapeutic invention. *Mol Cancer* 6:24–39.
27. Larrea MD, Wander SA, Slingerland JM (2009) p27 as Jekyll and Hyde: Regulation of cell cycle and cell motility. *Cell Cycle* 8:3455–3461.
28. Hofmann MC, Narisawa S, Hess RA, Millán JL (1992) Immortalization of germ cells and somatic testicular cells using the SV40 large T antigen. *Exp Cell Res* 201:417–435.
29. Danno S, Itoh K, Matsuda T, Fujita J (2000) Decreased expression of mouse Rbm3, a cold-shock protein, in Sertoli cells of cryptorchid testis. *Am J Pathol* 156:1685–1692.
30. Nakagawa T, Sharma M, Nabeshima Y, Braun RE, Yoshida S (2010) Functional hierarchy and reversibility within the murine spermatogenic stem cell compartment. *Science* 328:62–67.
31. Lleonart ME (2010) A new generation of proto-oncogenes: Cold-inducible RNA binding proteins. *Biochim Biophys Acta* 1805:43–52.
32. Hong JK, Kim YG, Yoon SK, Lee GM (2007) Down-regulation of cold-inducible RNA-binding protein does not improve hypothermic growth of Chinese hamster ovary cells producing erythropoietin. *Metab Eng* 9:208–216.
33. Lochhead PA, Sibbet G, Morrice N, Cleghon V (2005) Activation-loop autophosphorylation is mediated by a novel transitional intermediate form of DYRKs. *Cell* 121: 925–936.
34. Zou Y, Lim S, Lee K, Deng X, Friedman E (2003) Serine/threonine kinase Mirk/Dyrk1B is an inhibitor of epithelial cell migration and is negatively regulated by the Met adaptor Ran-binding protein M. *J Biol Chem* 278:49573–49581.
35. Lim S, Jin K, Friedman E (2002) Mirk protein kinase is activated by MKK3 and functions as a transcriptional activator of HNF1alpha. *J Biol Chem* 277:25040–25046.
36. Fotovati A, Nakayama K, Nakayama KI (2006) Impaired germ cell development due to compromised cell cycle progression in Skp2-deficient mice. *Cell Div* 1:4–13.
37. Nakayama K, et al. (1996) Mice lacking p27(Kip1) display increased body size, multiple organ hyperplasia, retinal dysplasia, and pituitary tumors. *Cell* 85:707–720.
38. Beumer TL, et al. (1999) Regulatory role of p27kip1 in the mouse and human testis. *Endocrinology* 140:1834–1840.
39. Kanatsu-Shinohara M, Takashima S, Shinohara T (2010) Transmission distortion by loss of p21 or p27 cyclin-dependent kinase inhibitors following competitive spermatogonial transplantation. *Proc Natl Acad Sci USA* 107:6210–6215.
40. Kim JK, Diehl JA (2009) Nuclear cyclin D1: An oncogenic driver in human cancer. *J Cell Physiol* 220:292–296.
41. Beumer TL, Roepers-Gajadien HL, Gademan IS, Kal HB, de Rooij DG (2000) Involvement of the D-type cyclins in germ cell proliferation and differentiation in the mouse. *Biol Reprod* 63:1893–1898.
42. Deng X, Ewton DZ, Pawlikowski B, Maimone M, Friedman E (2003) Mirk/dyrk1B is a Rho-induced kinase active in skeletal muscle differentiation. *J Biol Chem* 278: 41347–41354.

Supporting Information

Masuda et al. 10.1073/pnas.1121524109

SI Materials and Methods

Generation of Cold-Inducible RNA-Binding Protein (Cirp)-Deficient Mice. The targeting vector, pKO-Cirp, was electroporated into D3 ES cells and selected with G418 and gancyclovir. The targeting events were screened by PCR and confirmed by Southern blot analysis using several restriction endonucleases and both 3′ and 5′ end probes. The recombinant cells were karyotyped to ensure that 2N chromosomes were present in the majority of the metaphase spreads. Chimeric mice, which were derived from correctly targeted ES cells, were mated to C57BL/6 mice to obtain F1 *cirp*$^{+/-}$ mice. Germ-line transmission of the mutant allele was achieved from male chimeras. The mutant mice were backcrossed to C57BL/6 mice at least seven generations before being used in the experiments. All animal experiments were reviewed and approved by the Animal Committee of Kyoto University.

Antibodies. Rabbit polyclonal anti–dual-specificity tyrosine-phosphorylation–regulated kinase 1B (Dyrk1b) antibody was raised against peptides corresponding to the C-terminal 10 aa of mouse Dyrk1b and affinity-purified before use. Rabbit polyclonal antibodies recognizing the C terminus of mouse Cirp and mouse RNA-binding motif protein 3 (Rbm3) were prepared as described (1, 2). For biotinylation of the antibodies, antisera were purified by absorption to protein G, biotinylated, and then affinity-purified.

The sources of commercial antibodies were as follows: Phycoerythrin-conjugated anti–α6-integrin (G0H3) and anti-epithelial cell adhesion molecule (EpCAM) (G8.8) antibodies as well as FITC-conjugated anti-Ki67 (B56) antibody and phycoerythrin-conjugated anti-CD34 (RAM34) monoclonal antibodies were from BD Pharmingen; allophycocyanin-conjugated anti–Sca-1 (D7) and phycoerythrin/Cy7-conjugated anti–c-Kit (ACK2) monoclonal antibodies were from eBioscience; anti-BrdU monoclonal antibody (Bu20) was from DAKO; anti-FLAG M2 and biotinylated anti-HA (12CA5) monoclonal antibodies were from Sigma; anti-HA monoclonal antibody (F-7) and polyclonal antibodies to actin, p27/kip1, cyclin D1, and p16 were from Santa Cruz Biotechnology; Dyrk1b was from Cell Signaling Technology; allophycocyanin-conjugated streptavidin was from BD Pharmingen; swine TRITC-conjugated anti-rabbit IgG polyclonal antibody was from DAKO; and Cytox Green was from Molecular Probes.

Anti-lineage monoclonal antibodies Gr-1, Mac-1, CD4, CD8, B220, and TER-119 as well as antibodies to CD45.1 and CD45.2 were purified from supernatants of cultured hybridomas RB6-8C5, M1/70, GK1.5, 53-6.72, RA3-6B2, TER-119, A20.1.2, and ALI4A2, respectively, by absorption to protein G and were biotinylated or conjugated with FITC or Alexa Fluor 647 (Molecular Probes). FITC-conjugated anti-rat IgGκ (K4F5; Coulter), HRP-conjugated goat anti-rabbit, or rabbit anti-goat IgG polyclonal antibodies (DAKO) were used as secondary antibodies.

Plasmids. pIRESneo2-EF1 and pIRESpuro2-EF1 plasmids were constructed by replacing the CMV promoter of pIRESneo2 and pIRESpuro2 (Clontech) with EF1α promoter, respectively. pIRESbsr2-EF1 was constructed by replacing the neomycin-resistance gene of pIRESneo2-EF1 with the blasticidin-resistance gene. The reverse tetracycline-responsive transcriptional activator (rtTA) expression vector pBsr2-EF1/rtTA was constructed by cloning a fragment containing rtTA, IRES, and the tetracycline-regulated repressor tTS(kid) from Bs/IRES-M2 (1) into pIRESbsr2-EF1. The tetracycline-repressor (TR) expression vectors pIRESneo2-EF1/TR and pIRESpuro2-EF1/TR were constructed by cloning the TR from pcDNA6/TR (Invitrogen) into pIRESneo2-EF1 and pIRESpuro2-EF1, respectively.

pFRT/TRE/mCirp was constructed by replacing the CMV promoter of pcDNA/FRT (Invitrogen) with tandem repeats of tetracycline-responsive elements and CMV minimal promoter followed by insertion of mouse *cirp* cDNA into the multicloning site. For constructing pFRT/shCirp-1 and pFRT/shCirp-2 plasmids, the CMV promoter and poly(A) signal region of pcDNA/FRT were replaced with tandem repeats of mutated H1 promoter and oligonucleotides expected to generate siRNAs of the following sequences: shCirp-1, 5′-uuguguguagcauaacugucau-3′; and shCirp-2, 5′-uucggagaucugcccauac-3′. To stably down-regulate Dyrk1b expression, pPuro2/shDyrk-1 and pPuro2/shDyrk-2 plasmids were constructed that contained the puromycin-resistance gene driven by the SV40 promoter and tandem repeats of mutated H1 promoter and oligonucleotides expected to generate siRNAs of the following sequences: shDyrk-1, 5′-gcuguaucgguaggcucug-3′; and shDyrk-2, 5′-uaagagagucaaucucauagc-3′. To stably down-regulate Cirp or Dyrk1b expression, MSCV- or FMEV-based retroviral vectors containing the microRNA-30 backbone, MSCV-TMP/Cirp-i-1, and MSCV-TMP/Cirp-i-2 or SF2/Dyrk1b-i-1 and SF2/Dyrk1b-i-2 were constructed that generate the following RNA interfering sequences: Cirp-i-1, 5′-ucuccgaaguggugguguaaa-3′; and Cirp-i-2, 5′-uccuacagagacagctatgaca-3′; or Dyrk1b-i-1, 5′-agctatgagattgactctctaa-3′; and Dyrk1b-i-2, 5′-accagcggatctaccagtatat-3′, respectively.

Cells. Cirp(−/−)/teton-Cirp clones 2, 5, and 6 (Cl. 2, Cl. 5, and Cl. 6, respectively) were generated by cotransfecting mouse embryonic fibroblasts (MEFs) of the *cirp*$^{-/-}$ genotype first with pFRT/LacZeo (Invitrogen) and pBsr2-EF1/rtTA and then with pFRT/TRE/mCirp and pOG44 (Invitrogen). Cirp(+/+)/teton-shCirp-1, Cirp(+/+)/teton-shCirp-2, and Cirp(+/+)/teton-shSCR cells were generated by cotransfecting MEFs of the *cirp*$^{+/+}$ genotype first with pFRT/LacZeo and pIRESneo2-EF1/TR and then with pFRT/shCirp and pOG44. These cells were cultured in DMEM supplemented with 10% (vol/vol) calf serum, 100 μg/mL hygromycin, and 2 μg/mL blasticidin or 400 μg/mL G418. Cirp(+/+)/teton-shCirp-1 cells were further transfected with plasmids expressing shRNAs to Dyrk1b or scrambled sequences, or none (vector alone), and cultured in DMEM supplemented with 10% calf serum, 100 μg/mL hygromycin, 2.0 μg/mL puromycin, and 2 μg/mL blasticidin. The cells were cultured at 32 °C in a 5% CO_2, 95% air atmosphere unless indicated. HEK293T, U-2 OS, and HeLa cells were cultured in DMEM supplemented with 10% (vol/vol) FCS. PC3 cells were cultured in RPMI medium 1640 supplemented with 10% (vol/vol) FCS. MEF, NIH/3T3, and BALB/3T3 cells were cultured in DMEM supplemented with 10% (vol/vol) calf serum. All cells were cultured at 37 °C or 32 °C in a 5% CO_2, 95% air atmosphere.

GC-1spg cells were transduced with retroviral vectors MSCV-TMP/Cirp-i-1 or MSCV-TMPCirp-i-2 to down-regulate expression of Cirp and cultured in DMEM supplemented with 10% (vol/vol) calf serum and 2.0 μg/mL puromycin. To down-regulate expression of Dyrk1b, these cells were further transduced by retroviral vectors SF2/Dyrk1b-i-1 or SF2/Dyrk1b-i-2 and cultured with 2.0 μg/mL puromycin and 5 μg/mL blasticidin.

To estimate the protein degradation rate, cycloheximide was added to the culture media (final concentration of 100 μg/mL), and cells were harvested at different time points, pelleted by centrifugation, and analyzed by Western blotting (IB). Intensities

of the bands were quantified by scanning densitometry and normalized to those of β-actin at each point.

Primers for PCR. RT-PCR was performed with the following sets of primers: for actin, 5′-tcagaaggactcctatgtgg-3′ and 5′-tctctttgatgtcacgcacg-3′; for Cirp, 5′-aagtggtggtggtaaaggacag-3′ and 5′-atggaaggacgatctggacg-3′; for Dyrk1b, 5′-atcatccactgcgacctcaag-3′ and 5′-cctggtaatccttcctgagttc-3′; for p27, 5′-aacgtgcgagtgtctaacgg-3′ and 5′-gccgtgtcctcagagttagcc-3′; and for cyclin D1, 5′-gcgtgcagaaggagattgtgccat-3′ and 5′-atgaaatcgtggggagtcatggcg-3′.

The primer sets for quantitative PCR were as follows: for actin, 5′-gaaccctaaggccaaccgtgaaa-3′ and 5′-acagggacagcacagcctgga-3′; for p27, 5′-ctttaattgggtctcaggcaaactc-3′ and 5′-tgcgaagaagaatcttctgcagcag-3′; for cyclin D1, 5′-gctaccgcacaacgcactttctttc-3′and 5′-agcacaggtatcaggtaacagggct-3′; and for Rbm3, 5′-aacaccgatgaacaggcacttgaag-3′ and 5′-tagctctcatcgcatctgagg-3′.

To genotype the mice, genomic DNAs were extracted from tails and analyzed by PCR. To discriminate between wild-type and mutated alleles, the following sets of primers were used (a and b in Fig. 1 *A* and *B*): for wild-type locus, 5′-atagtccaggatggccttggaacac-3′ and 5′-gggatcaaaggcatataccaccatgtcc-3′; and for targeted locus, 5′-gcttcgtgaagccaaagaaactgcgtaca-3′ and 5′-gcccagaaagcgaaggagcaaag-3′.

Analysis of Spermatogonia. To isolate spermatogonia, dissociated testicular cells were first stained with anti-EpCAM monoclonal antibody and then FITC-conjugated anti-rat IgGκ antibody. EpCAM is a marker for spermatogonia in adult mouse testis (3). Stained cells were further stained with Alexa Fluor 647-conjugated anti–c-Kit monoclonal antibody and phycoerythrin-conjugated anti–α6-integrin monoclonal antibody to differentiate undifferentiated and differentiating spermatogonia and analyzed or sorted by FACS Aria (Becton Dickinson Immunocytometry System). Each time, two to eight mice were used per group. In some experiments, mice were injected i.p. with busulfan (30 mg/kg) and then killed at the indicated times.

Cell-Cycle Analysis. To detect cells undergoing DNA synthesis, BrdU was added to culture media (final concentration of 10 mg/mL) at 30 min before harvest. The harvested cells were fixed, treated with HCl, neutralized, stained with an anti-BrdU monoclonal antibody, and further stained with propidium iodide. BrdU incorporation and DNA content were analyzed on a flow cytometer (EPICS XL; Coulter). Sub-G1 population was evaluated by flow cytometry and cell-cycle analysis after permeabilization and staining with propidium iodide.

To detect cells that were not in cell cycle, flow cytometry was performed after cells were fixed and stained with FITC-conjugated anti-Ki67 monoclonal antibody and propidium iodide or stained with pyronin Y (4).

Yeast Two-Hybrid Screening. Full-length mouse *cirp* cDNA was subcloned into pGBKT7 (Clontech) and used as bait to screen a mouse testis cDNA library (Clontech).

Immunoprecipitation and Competitive Binding Assays. For coimmunoprecipitation of exogenous Cirp and Dyrk1b, plasmids pME18S/3Flag-Dyrk1b and pGFP/Cirp were cotransfected into HEK293T cells. At 48 h later, cell lysates were prepared with buffer containing 0.5% Nonidet P-40, immunoprecipitated with anti-FLAG or anti-GFP monoclonal antibody, and analyzed by IB using anti-GFP or anti-FLAG antibody, respectively. To detect coimmunoprecipitation of endogenous proteins, MEFs cultured at 32 °C were lysed with the Nuclear Co-IP kit (Active Motif), and immunoprecipitants prepared with anti-Dyrk1b antibody or Ig (control) and protein G Sepharose beads (GE Healthcare) were analyzed by IB.

To assess the effect of Cirp on the binding of Dyrk1b to p27 or cyclin D1, pME18S/3Flag-Dyrk1b was cotransfected with pIRESpuro2-EF1/Cirp, pIRESpuro2-EF1 (control vector), pCMV4-3HA2/cyclin D1, and pCMV4-3HA2/p27 in various combinations into HEK293T cells. Cell lysates were immunoprecipitated with anti-FLAG antibody and analyzed by IB.

In Vitro Kinase Assay. Immunoprecipitants were prepared with anti-FLAG antibody and protein G Sepharose beads from HEK293T cells transfected with pME18S/3Flag-mDyrk1b. They, or recombinant Dyrk1b proteins produced in *Escherichia coli*, were used as kinase. The kinase was incubated in the kinase buffer with [γ-^{32}P]ATP, recombinant GST-p27, GST-cyclin D1, or GST alone as substrate and varying amounts of GST-Cirp or 6xHis-Cirp. After the reaction, products were analyzed by SDS/PAGE and autoradiography. In some experiments, reaction mixtures were analyzed by SDS/PAGE and Coomassie blue staining or reaction mixtures without ^{32}P were analyzed by IB with or without prior precipitation with protein G Sepharose or glutathione Sepharose beads (GE Healthcare).

Histological and Immunocytochemical Analyses. Testis was fixed with paraformaldehyde and embedded in paraffin. Mounted sections were deparaffinized, rehydrated, and stained with hematoxylin and eosin. For immunocytochemical analysis, cells were stained with labeled antibodies and analyzed by a laser-scanning confocal microscope (FluoView; Olympus).

Analysis of Hematopoietic Stem Cells. Mononuclear cells were purified from mouse bone marrow cells with Pancoll (PAN Biotech) and stained with monoclonal anti-lineage antibodies followed by FITC-conjugated anti-rat IgGκ monoclonal antibody and anti–Sca-1, anti–c-Kit, and anti-CD34 monoclonal antibodies. Then FACS Aria analysis was performed.

Competitive Reconstitution Assay for Hematopoiesis. Sublethally irradiated C57BL/6-CD45.1 mice were i.v. transplanted with 5×10^5 bone marrow cells from Cirp-deficient or littermate wild-type mice (CD45.2) together with 5×10^5 cells from C57BL/6-CD45.1 mice as a competitor (Fig. S1*C*). Percentage of CD45.2$^+$ cells in the peripheral blood was analyzed at 16 wk after transplantation. These recipient mice were irradiated (4.5 Gy) again, and the percentage of CD45.2$^+$ cells were analyzed at 4 and 16 wk later.

Data Analysis. All of the statistical analyses were done by Student's *t* test with the JMP statistical software package (SAS Institute).

1. Nishiyama H, et al. (1997) A glycine-rich RNA-binding protein mediating cold-inducible suppression of mammalian cell growth. *J Cell Biol* 137:899–908.
2. Danno S, Itoh K, Matsuda T, Fujita J (2000) Decreased expression of mouse Rbm3, a cold-shock protein, in Sertoli cells of cryptorchid testis. *Am J Pathol* 156:1685–1692.
3. Anderson R, Schaible K, Heasman J, Wylie C (1999) Expression of the homophilic adhesion molecule, Ep-CAM, in the mammalian germ line. *J Reprod Fertil* 116:379–384.
4. Deng X, Ewton DZ, Friedman E (2009) Mirk/Dyrk1B maintains the viability of quiescent pancreatic cancer cells by reducing levels of reactive oxygen species. *Cancer Res* 69:3317–3324.

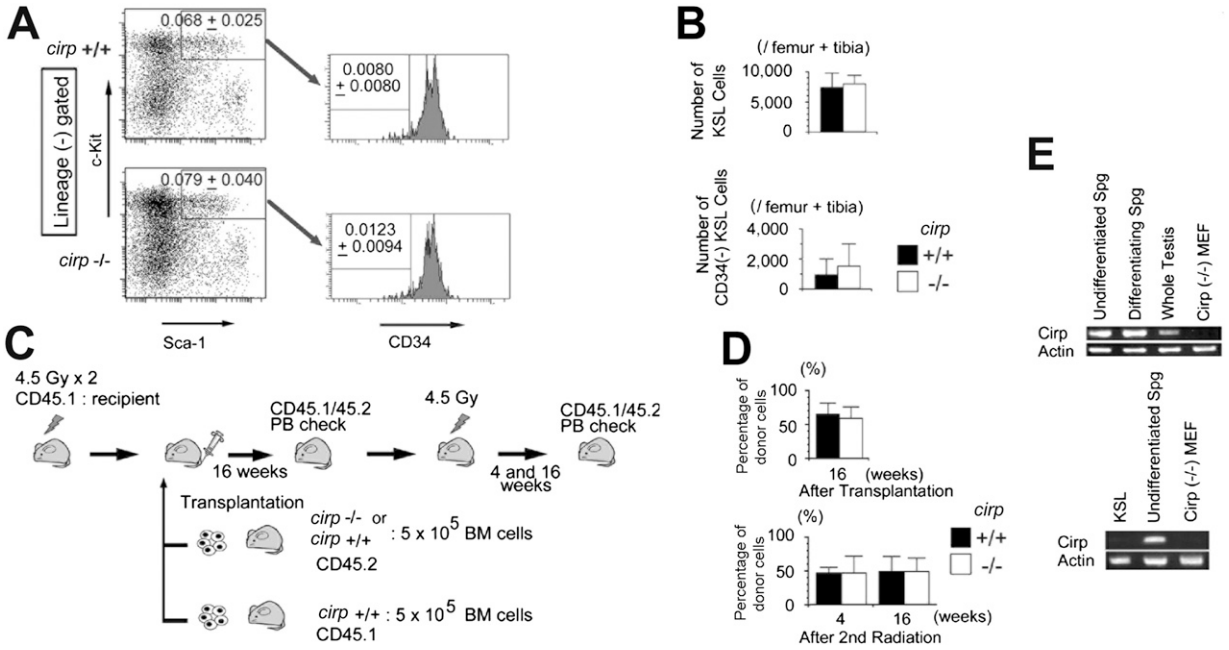

Fig. S1. Hematopoietic stem cells in *cirp*-knockout mice. (*A*) Percentage of c-Kit$^+$Sca-1$^+$Lin$^-$ (KSL) and CD34$^-$ KSL cells in Lin$^-$ bone marrow cells of *cirp*$^{+/+}$ (+/+) and *cirp*$^{-/-}$ (–/–) mice analyzed by flow cytometry. No significant difference was found between +/+ and –/– mice in the percentage of KSL ($P = 0.64$) or CD34$^-$ KSL ($P = 0.48$) fraction. Representative data are of four +/+ and five –/– mice. (*B*) Numbers of KSL and CD34$^-$ KSL cells. No significant difference was found between +/+ and –/– mice in the numbers of cells in KSL ($P = 0.45$) or CD34$^-$ KSL ($P = 0.49$) fraction. Values represent mean ± SD ($n = 4$). (*C*) Schematic illustration of the competitive reconstitution assay of hematopoiesis. BM, bone marrow; PB, peripheral blood. (*D*) Percentage of CD45.2 donor cells in peripheral blood of CD45.1 recipient mice. No significant difference was found between +/+ and –/– mice at 16 wk after transplantation ($P = 0.68$) or at 4 or 16 wk after second irradiation ($P = 1.0$ and 0.90, respectively). Values represent mean ± SD ($n = 3$). (*E*) Detection of *cirp* expression in spermatogonia but not in the KSL fraction. RNAs prepared from indicated sources were analyzed by RT-PCR.

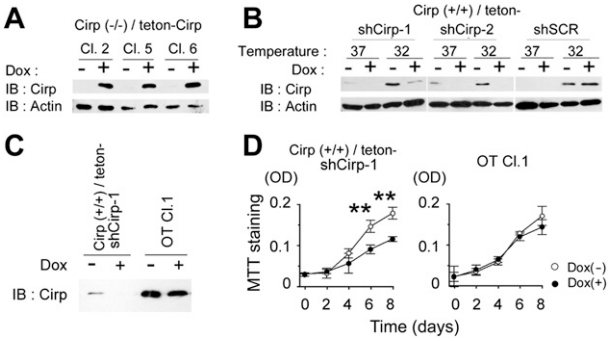

Fig. S2. Modulation of Cirp protein level and cell growth in MEFs. (*A*) Cells from Cirp(–/–)/teton-Cirp Cl. 2, Cl. 5, and Cl. 6 were derived from *cirp*$^{-/-}$ MEFs. They were cultured at 37 °C in the presence or absence of doxycycline (Dox), and the cell lysates were analyzed by IB using the indicated antibodies. (*B* and *C*) Cirp(+/+)/teton-shCirp cells are derived from *cirp*$^{+/+}$ MEFs that inducibly express shRNAs that target *cirp* RNAs (shCirp-1 and shCirp-2) or scrambled RNAs (shSCR). OT Cl. 1 cells are derived from Cirp(+/+)/teton-shCirp-1 cells that stably express *cirp* mRNA that have a mutation within the shRNA target sequence but encode wild-type Cirp protein. Cells were cultured at the indicated temperatures (*B*) or at 32 °C (*C*) and analyzed as in *A*. (*D*) Proliferation of Cirp(+/+)/teton-shCirp-1 cells and OT Cl. 1 cells in the presence (+) or absence (–) of Dox at 32 °C. Cell numbers were assessed by 3-(4,5-dimethylthiazol-2-yl)-2,5-diphenyltetrazolium bromide (MTT) assays. Values are mean ± SD ($n = 3$). *$P < 0.05$. **$P < 0.01$.

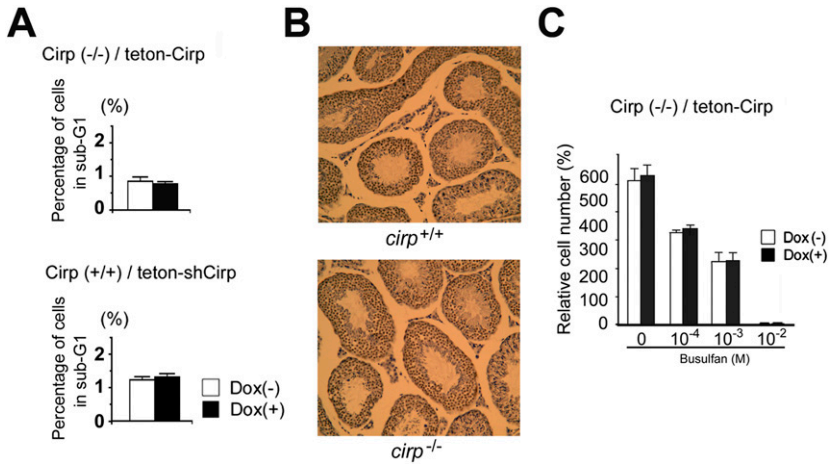

Fig. S3. Effects of Cirp on apoptosis. (*A*) Percentage of cells in sub-G1 phase. DNA content was analyzed in the indicated cells cultured at 32 °C in the presence (+) or absence (–) of Dox as in Fig. 2*C*. Values are mean ± SD (n = 3). (*B*) Identification of apoptotic cells in the testes. Testes of $cirp^{+/+}$ and $cirp^{-/-}$ mice were fixed in phosphate-buffered formalin and embedded in paraffin at 2 wk after injection of busulfan. Mounted sections were deparaffinized and rehydrated, and apoptotic cells were identified by the TUNEL method. (*C*) Cytotoxic effects of busulfan. Cirp(–/–)/teton-Cirp Cl. 5 cells were cultured for 3 d with busulfan at the indicated concentrations in the presence (+) or absence (–) of Dox at 37 °C. Cell numbers were assessed by MTT assays and expressed as relative to those at the start of the treatment. Values are mean ± SD (n = 3).

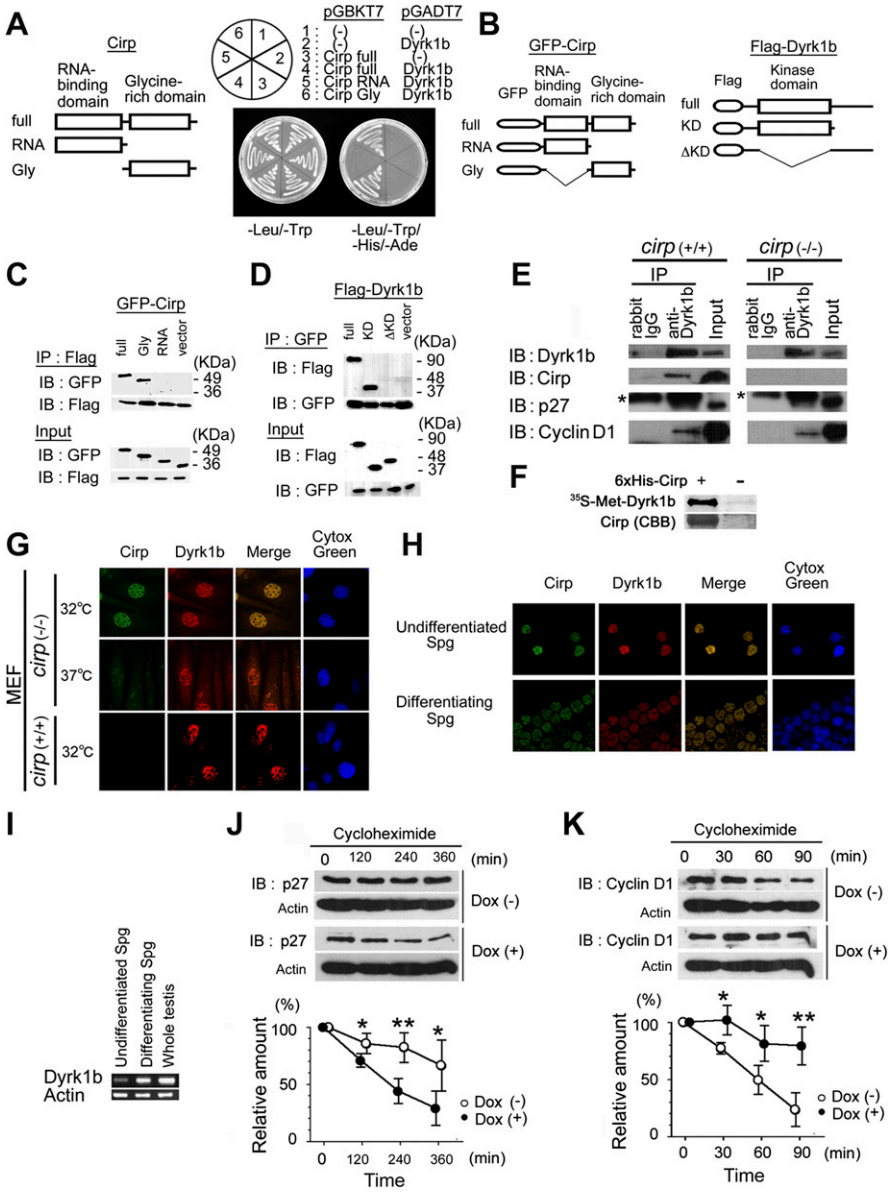

Fig. S4. Binding of Cirp to Dyrk1b and its effects on degradation of p27 and cyclin D1. (*A*) Binding of the glycine-rich domain of Cirp to Dyrk1b in yeasts. (*Left*) Schema of constructs expressing wild-type Cirp (full) or mutant Cirp (RNA and Gly). (*Right*) Yeasts were transformed with combinations of plasmids as indicated, cultured in the selection media, and photographed. (*B*) Schema of constructs expressing GFP-fused Cirp, wild-type (full), RNA-binding domain alone (RNA), or glycine-rich domain alone (Gly) and FLAG-tagged Dyrk1b, wild-type (full), kinase domain alone (KD) or kinase domain deleted (ΔKD). (*C* and *D*) Necessity of the glycine-rich domain of Cirp and the kinase domain of Dyrk1b for interaction. HEK293T cells were cotransfected with plasmids expressing FLAG-Dyrk1b and GFP-fused Cirp mutants (*C*) or plasmids expressing GFP-Cirp and FLAG-tagged Dyrk1b mutants (*D*) as indicated. Cell lysates were immunoprecipitated (IP), and precipitants and inputs were analyzed by IB using the indicated antibodies. Experiments were repeated twice, with similar results. (*E*) Coimmunoprecipitation (IP) of endogenous Dyrk1b protein with Cirp, p27, and cyclin D1. Cell lysates prepared from MEFs derived from $cirp^{+/+}$ and $cirp^{-/-}$ mice cultured at 32 °C were precipitated with anti-Dyrk1b antibody or normal rabbit IgG and analyzed along with inputs (5%) by IB using the indicated antibodies. *Light chain of IgG. (*F*) In vitro-translated ^{35}S-labeled Dyrk1b was mixed with nickel–nitrilotriacetic acid (Ni-NTA) resin in the presence (+) or absence (–) of recombinant His-tagged Cirp, and precipitants were analyzed by fluorography after separation by SDS/PAGE. CBB, Coomassie blue staining. (*G*) Immunocytochemical analysis of Cirp and Dyrk1b in $cirp^{+/+}$ and $cirp^{-/-}$ MEFs. Cells cultured at the indicated temperatures were stained with anti-Cirp (green) and anti-Dyrk1b (red) antibodies and observed under the confocal microscope. Nuclei were stained with Cytox Green. (*H*) Immunocytochemical analysis of Cirp and Dyrk1b expression in undifferentiated spermatogonia. The cells were isolated from $cirp^{+/+}$ mice and analyzed as in *G*. (*I*) Expression of Dyrk1b mRNA in undifferentiated spermatogonia from $cirp^{+/+}$ mice. RNAs prepared from the indicated sources were analyzed by RT-PCR using the indicated primers. (*J* and *K*) Effects of Cirp on stability of p27 and cyclin D1 proteins. Cirp(–/–)/teton-Cirp Cl. 5 cells that express Cirp in the presence of Dox were cultured in the presence (+) or absence (–) of Dox. At the indicated times after addition of cycloheximide to the culture medium, cells were harvested and cell lysates were analyzed by IB using the indicated antibodies. To quantify the amount, blot images (representative data; upper blots) were scanned by a densitometer and normalized to actin levels (lower blots). Values represent mean ± SD (n = 4). *$P < 0.05$. **$P < 0.01$.

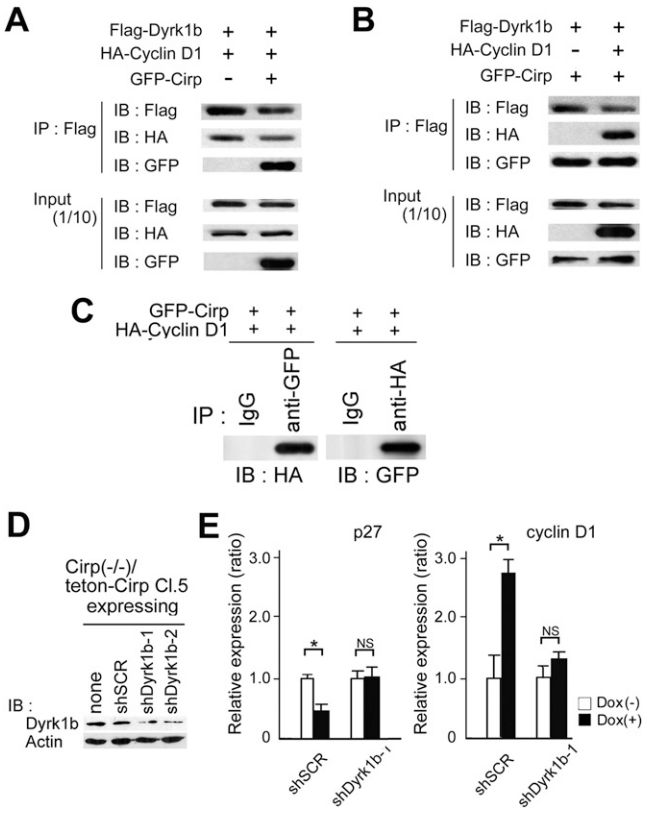

Fig. S5. Coimmunoprecipitation of Cirp with cyclin D1 and Dyrk1b and Dyrk1b dependency of Cirp function. (*A*) Effects of Cirp on binding of Dyrk1b to cyclin D1. HEK293T cells were cotransfected with plasmids expressing the indicated proteins (+) or a control vector (–). Cell lysates were immunoprecipitated (IP) with anti-FLAG antibody. Precipitants and inputs were analyzed by IB using the indicated antibodies. (*B*) Effects of cyclin D1 on binding of Dyrk1b to Cirp. HEK293T cells were cotransfected with plasmids expressing the indicated proteins (+) or a control vector (–). Cell lysates were immunoprecipitated (IP) with anti-FLAG antibody. Precipitants and inputs were analyzed by IB using the indicated antibodies. (*C*) Coimmunoprecipitation (IP) of cyclin D1 and Cirp. HEK293T cells were cotransfected with plasmids expressing the indicated proteins. Cell lysates were immunoprecipitated with anti-GFP antibody, anti-HA antibody, or normal IgG and analyzed by IB using the indicated antibodies. (*D*) Effects of shRNAs. Cirp(–/–)/teton-Cirp Cl. 5 cells stably expressing shRNAs to Dyrk1b (shDyrk1b-1 and shDyrk1b-2), scrambled sequences (shSCR), or vector alone (none) were cultured at 37 °C. Cell lysates were analyzed by IB using the indicated antibodies. (*E*) Dyrk1b-dependent effects of Cirp on protein levels of p27 and cyclin D1. shSCR and shDyrk1b-1 cells were cultured at 37 °C in the presence (+) or absence (–) of Dox. Cell lysates were analyzed by IB using anti-p27, anti-cyclin D1, anti-Cirp, and anti–β-actin antibodies. A representative result is shown in Fig. 4*B*. To quantify the amount, blot images were scanned by a densitometer and normalized to actin levels. The normalized protein level was expressed as relative to that in cells cultured in the absence of Dox. Values represent mean ± SD (n = 4). *P < 0.01. NS, not significant.

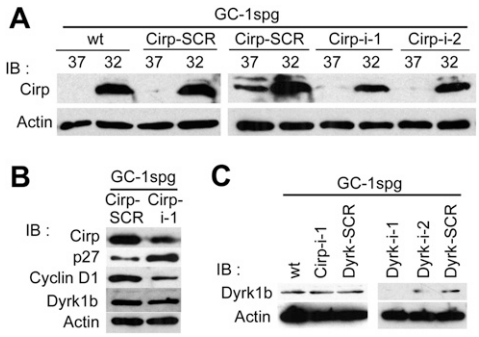

Fig. S6. Down-regulation of Cirp and Dyrk1b expression in the mouse spermatogonial cell line GC-1spg. (*A*) Suppression of Cirp expression. GC-1spg cells were transduced with retroviruses (MSCV-TMP) expressing RNAi sequences targeted to Cirp (Cirp-i-1 and Cirp-i-2), scrambled RNAs (Cirp-SCR), or none (wt) and cultured in the presence of 2.0 μg/mL puromycin at the indicated temperatures. Cell lysates were analyzed by IB using the indicated antibodies. (*B*) Lysates from indicated cells cultured at 32 °C were analyzed by IB using the indicated antibodies. (*C*) Suppression of Dyrk1b expression. Cirp-i-1 cells were further transduced with retroviruses (SF2) expressing RNAi against Dyrk1b (Dyrk-i-1 and Dyrk-i-2) or scrambled RNAs (Dyrk-SCR). After transduction, cells were cultured in the presence of 2.0 μg/mL puromycin and 5 μg/mL blasticidin, and their lysates were analyzed by IB using the indicated antibodies.

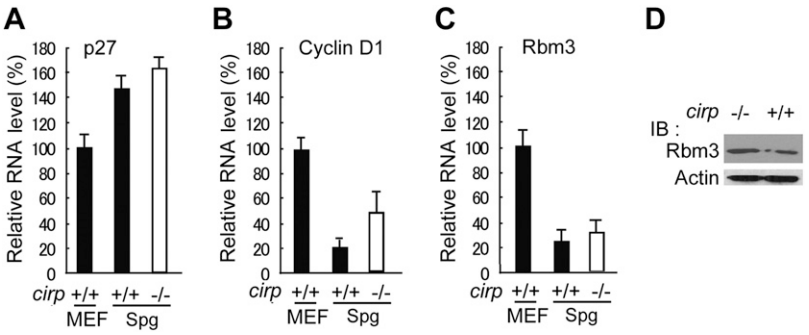

Fig. S7. RNA levels of p27, cyclin D1, and Rbm3 in spermatogonia. (*A*–*C*) Undifferentiated spermatogonia of *cirp*$^{-/-}$ and *cirp*$^{+/+}$ genotypes were sorted and analyzed at 4 wk after busulfan treatment. cDNAs were prepared from sorted spermatogonia and *cirp*$^{+/+}$ MEFs and analyzed by quantitative RT-PCR using specific primers for the indicated genes. Values are mean ± SD of triplicates (n = 3). (*D*) Protein levels of Rbm3. EpCAM^{+} testicular cells were purified by flow cytometry from two mice each of the *cirp*$^{-/-}$ and *cirp*$^{+/+}$ genotypes. Cell lysates were analyzed by IB using the indicated antibodies. Experiments were repeated twice, with similar results.

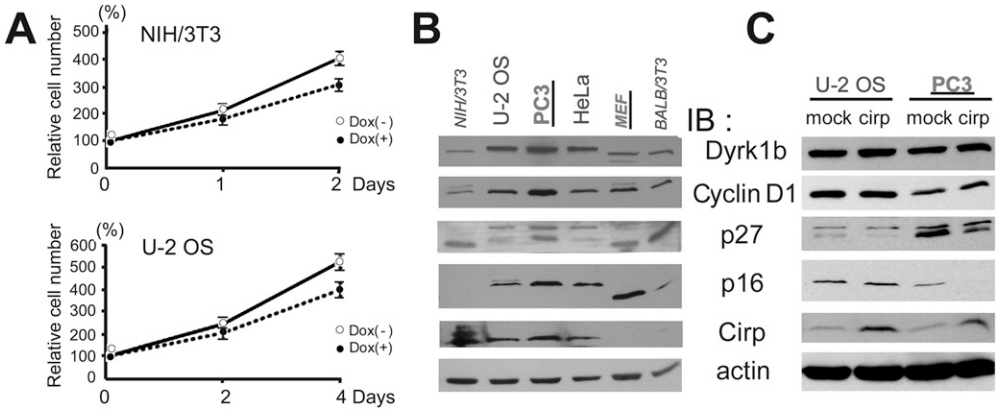

Fig. S8. Effects of Cirp expression on proliferation and gene expression in various cell lines. (*A*) Suppressive effects of Cirp on proliferation of cells. NIH/3T3 cells and U-2 OS cells were engineered to express Cirp in the presence of Dox. They were cultured in the presence (+) or absence (–) of Dox at 37 °C. Cell numbers were assessed by MTT assays. Values are mean ± SD (n = 3). (*B*) Gene expression in the two classes of cell lines cultured to 80–90% confluent at 37 °C. Cell lysates were analyzed by IB using the indicated antibodies. Names of cell line whose proliferation is stimulated by Cirp are underlined, and those of mouse origin are italicized. (*C*) Effects of Cirp on gene expression. Indicated cells were transduced with lentivirus (pLVSIN-EF1α Pur Vector) expressing human Cirp or none (mock), cultured in selection media for 1 wk, and then analyzed as in *B*. Experiments were repeated twice (*B* and *C*), with similar results.

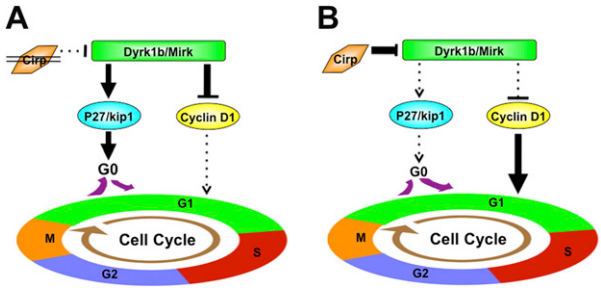

Fig. S9. Proposed mechanism by which Cirp stimulates cell-cycle progression. (*A*) In the absence of Cirp, Dyrk1b phosphorylates and blocks degradation of p27/kip1, which helps to maintain the quiescent G0 state. Dyrk1b also blocks cells from traversing the G1 phase of the cell cycle by phosphorylating and destabilizing cyclin D1. (*B*) Cirp binds to Dyrk1b and inhibits its kinase activity toward p27/kip1 and cyclin D1, resulting in cell-cycle progression.